J. Am. Soc. Mass Spectrom. (2018) 29:2096–2104
DOI: 10.1007/s13361-018-2014-y

RESEARCH ARTICLE

# Simulation of Unidirectional Ion Ejection in an Asymmetric Half-Round Rod Electrode Linear Ion Trap Mass Analyzer

HaiYan Wu, LiPeng Zhang, ZaiYue Zhang, Jie Qian, ShuGuang Zhang, YingJun Zhang, SaiJin Ge, XiaoXu Li

School of Mechanical and Electrical Engineering, Soochow University, Suzhou, 215021, China

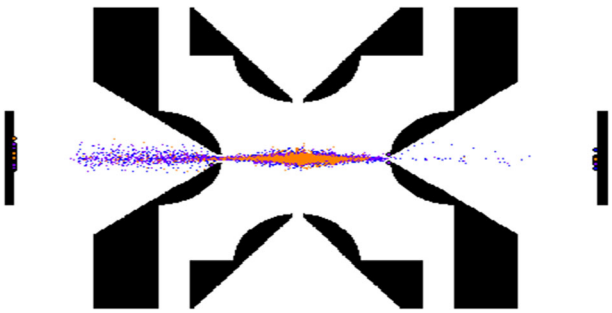

**Abstract.** An asymmetric trapping field was generated from an asymmetric half-round rod electrode linear ion trap (A-HreLIT), and its performance of unidirectional ion ejection was studied. Two different asymmetric structures of A-HreLITs were constructed, one rotating *y* electrode pairs toward an *x* electrode with an angle *θ*, and the other stretching one *x* electrode with a distance *α*. The center of trapping field was displaced away from the geometrical center of the ion trap, defined to be the midpoint along the axis of *y* between *x* electrodes, which leads to unidirectional ion ejection through one *x* electrode. Computer simulations were used to investigate the relationship between asymmetric geometric parameter of *θ* (or *α*) and analytical performance. Both structures could result in similar asymmetric trapping fields, which mainly composed of dipole, quadrupole, and hexapole fields. The dipole and hexapole fields were approximately proportional to the asymmetric geometric parameter of rotation angle *θ* (or stretch distance *α*). In simulation, ion trajectories and ion kinetic energy were calculated. For ions with *m/z* 609 Th, the simulation results showed that mass resolution of over 2400 (FWHM) and ion unidirectional ejection efficiency of nearly 90% were achieved in an optimized A-HreLIT. Ion detection efficiency of A-HreLIT could be improved significantly with only one ion detector, while maintaining a considerable mass resolution. Furthermore, the A-HreLIT could be driven by a traditional balanced RF power supply. These advantages make A-HreLIT suitable for developing miniaturized mass spectrometer with high performance.

**Keywords:** Unidirectional ion ejection, Asymmetric geometry, Ion detection efficiency, Miniaturization, Odd-order fields

Received: 10 April 2018/Revised: 19 June 2018/Accepted: 19 June 2018/Published Online: 11 July 2018

## Introduction

A linear ion trap (also referenced as two-dimensional ion trap) could mainly be divided into an axial ejection linear ion trap (AeLIT) [1, 2] and a radial ejection linear ion trap (ReLIT) [3] according to ion ejection direction during mass analysis. In recent years, various types of ReLIT with simplified geometry were developed for special purposes, such as a rectilinear ion trap (RIT) [4, 5], an ion trap array (ITA) [6], a triangular-electrode linear ion trap (TeLIT) [7, 8], a printed circuit board ion trap (PCBIT) [9] and a half-round rod electrode linear ion trap (HreLIT) [10], etc. The simplified ReLIT was considered to be more suitable for developing miniaturized mass spectrometer than classical ReLIT, due to its ease of fabrication, compact size, and low cost [11–13].

The performance of an ion trap, including mass resolution, sensitivity, spectrum scan speed, ion capacity, and collision-induced dissociation (CID) capabilities were studied in many previous works by means of experiment and simulation [3, 14, 15]. Performance improvement was usually achieved by optimizing the geometrical shape and relative position of electrodes. For example, "stretch" of electrodes was a widely used geometry optimizing method of enhancing mass resolution, which has been successfully applied on classical ReLIT [3], RIT [4], and HreLIT [10]. There were other methods, which focused on optimizing electrode shape, $r/r_0$ [16], and slot size [7], etc.

*Correspondence to:* XiaoXu Li; *e-mail:* xxli@suda.edu.cn

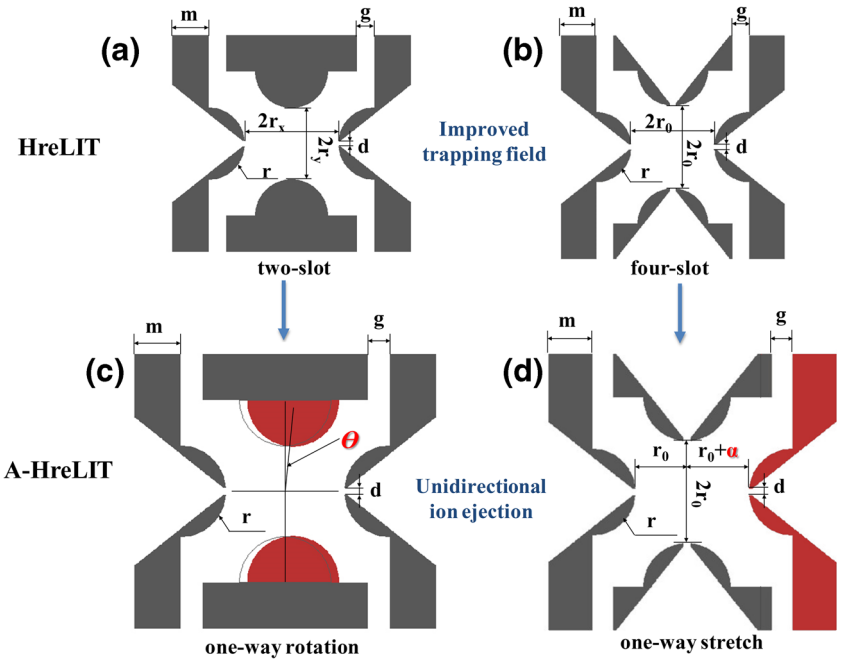


**Figure 1.** Construction of A-HreLIT: (**a**) cross-section of two-slot HreLIT; (**b**) cross-section of four-slot HreLIT; (**c**) cross-section of one-way rotated A-HreLIT; (**d**) cross-section of one-way stretched A-HreLIT

Computer simulation played a very important role in the process of studying and optimizing an ion trap. Mathematical modeling approaches have been proved useful, especially for deep understanding of some phenomenon observed in experiments, such as the relationship between mass resolution and scan speed [3, 14]. However, numerical simulations are required in study of scanning of RF field and "realistic" ion trap electrode geometries [17]. Especially for simplified structured ion traps, such as a cylindrical ion trap (CIT) [18–20], RIT, and TeLIT [7], the internal potential could hardly be expressed by strictly defined mathematical models. In such situations, numerical simulations were used to study ion trajectory, ion ejection process, and ion neutral collisions, and finally to evaluate the performance of these "realistic" ion traps.

Sensitivity is critical for mass spectrometer in real application. Ion capacity, ion ejection efficiency, and ion detection efficiency have great impacts on ultimate sensitivity of an ion trap mass spectrometer. For existed ReLITs, including RIT, ITA, TeLIT, and HreLIT, ions were ejected from both sides along the *x*-axis, which means that ion detection efficiency would not be higher than 50% if only one ion detector was used, as it usually does in miniaturized ion trap mass spectrometers. To solve this problem, two ion detectors were used in a commercialized LIT mass spectrometer (LTQ, Thermo Finnigan) [21]. However, this configuration requires a large vacuum chamber and high cost, which is undesirable for developing miniaturized mass spectrometers.

Ion detection efficiency could be greatly improved by unidirectional ion ejection even if only one detector was used. Splendore et al. [15] employed an asymmetric trapping field on a traditional three-dimensional ion trap by adding an alternating voltage out of phase to the endcap electrodes at the same frequency as the ring electrode. In this case, the center of ion vibration was displaced away from the geometrical center of the trap. Experiment results showed that unidirectional ion ejection occurred and the absolute ion abundance was doubled. Remes et al. [17] created several models of hyperbolic ReLITs with asymmetric geometry and studied their performance using numerical simulation approaches. These asymmetric ion traps were highly comparable to an ideal quadrupole ion trap in mass resolution. Wang et al. [22] studied the ion motion characteristics in a quadrupole ion trap coupling with hexapole and octopole fields using mathematical modeling approach. It was found that hexapole field leads to unidirectional ion ejection and degradation of mass resolution, while octopole field could compensate nonlinear effects and enhance mass resolution. In

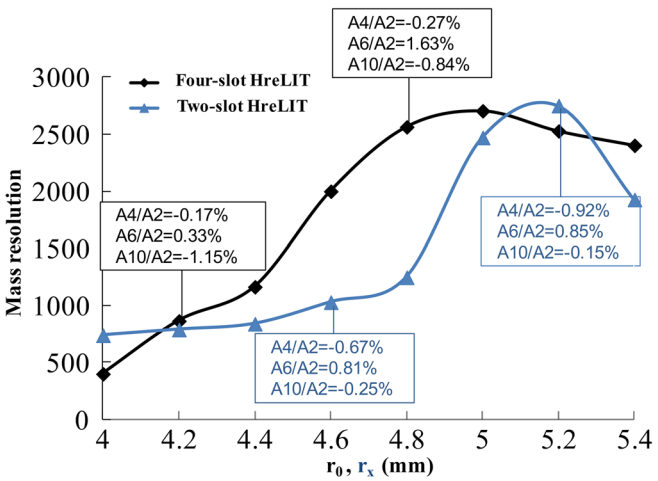


**Figure 2.** Mass resolution of two-slot HreLIT as a function of $r_x$ and mass resolution of the four-slot HreLIT as a function of $r_0$

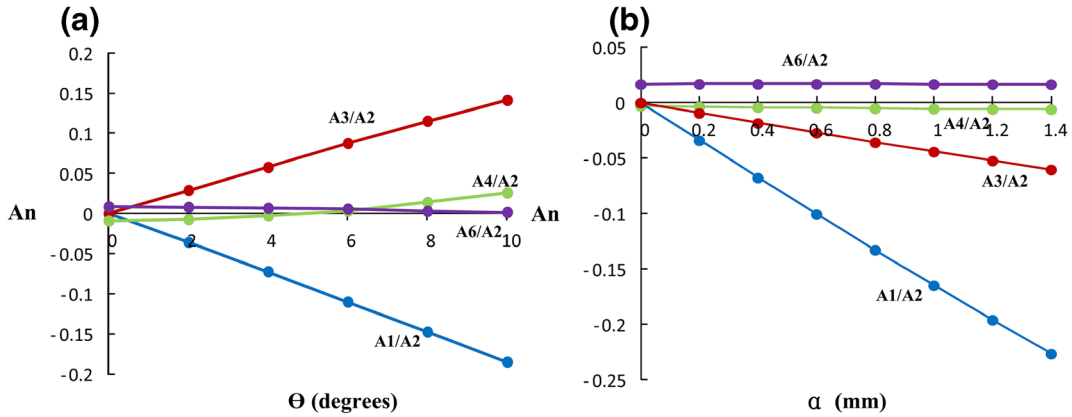


**Figure 3.** (**a**) Amplitudes of multipole components $A_N$ versus $\theta$ for one-way rotated A-HreLIT; (**b**) amplitudes of multipole components $A_N$ versus $\alpha$ for one-way stretched A-HreLIT

summary, it could concluded that asymmetric electric fields (odd-order fields) were the key to unidirectional ion ejection, and proper components of even-order fields were necessary for compensating the nonlinear effects and enhance mass resolution. The asymmetric electric fields could be added to an ion trap by applying unbalanced RF trapping voltage on electrodes or by constructing an ion trap with asymmetric geometries.

In the present study, two types of "realistic" models of A-HreLITs were created, and their performances including unidirectional ion ejection efficiency and mass resolution were studied using numerical simulation approaches. The impact of geometric parameters on performance was also studied.

## Simulation

### *Structure of a -HreLIT*

Two different A-HreLITs were constructed based on two types of HreLITs. The first type of HreLIT had two identical slots on the $x$ electrode pairs and was herein referred to as two-slot HreLIT, and the two $x$ electrodes were displaced away from the geometric center by a small distance. As shown in Fig. 1(c), the first structure of A-HreLIT (referred as one-way rotated A-HreLIT) was derived from the two-slot HreLIT by rotating two $y$ electrodes around the geometric center toward positive $x$-direction with an angle $\theta$. The second type of HreLIT had four identical slots on both $x$ and $y$ electrodes and was herein referred to as four-slot HreLIT. For four-slot HreLIT, the $x$ and $y$ electrode pairs were both displaced away from the geometric center by same distance, i.e., $r_x = r_y = r_0 \geq 4.0$ mm. And the second structure of A-HreLIT (referred as one-way stretched A-HreLIT) was derived from the four-slot HreLIT by stretching only one $x$ electrode by a distance $\alpha$.

The modeled ion trap electrode profiles were created using the SIMION 8.0 geometry file scripting language. A two-dimensional model was used in the simulation and was defined in cross-section with an 800-by-800 point grid array

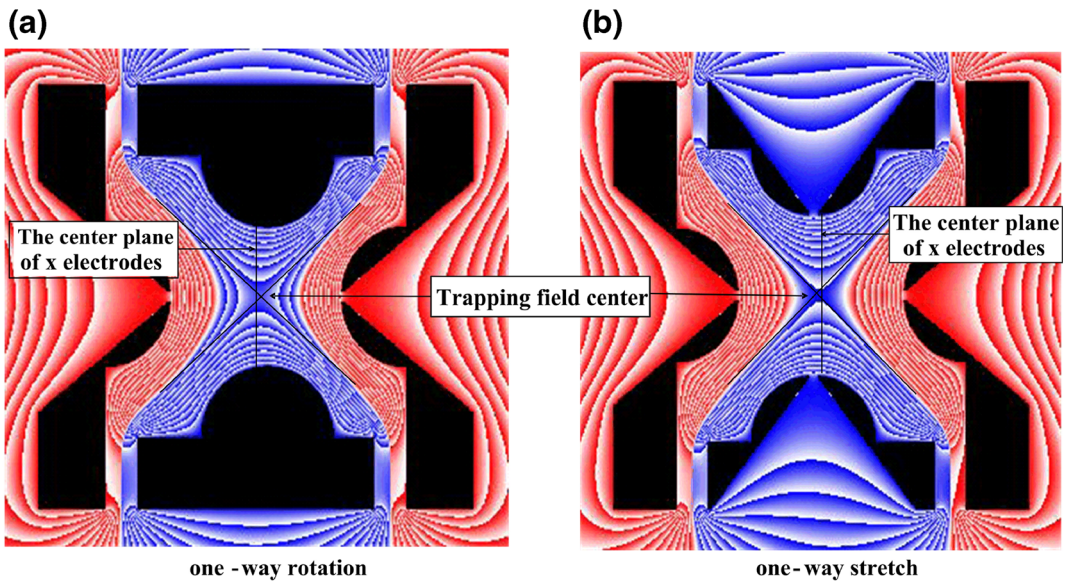


**Figure 4.** Equipotential lines in a trapping field: (**a**) the one-way rotated A-HreLIT with $\theta = 5°$; (**b**) the one-way stretched A-HreLIT with $\alpha = 1$ mm

with a grid step of 0.05 mm. The radius of the half-round rod $r = 4.0$ mm, the width of slots $d = 0.6$ mm, the gap between the $x$ and $y$ electrodes $g = 2.0$ mm and the width of the rectangular rod for mounting $m = 4.0$ mm.

## *Field and Ion Trajectory Simulation*

The performance of ion trap was mainly determined by its internal electric field distribution. Until now, there have been many studies focusing on quadrupole and high-order fields of ion trap [16]. In this study, the internal electric field of A-HreLIT was also studied.

Analysis of planar two-dimensional potential fields is based on the fact that, in region without electrodes, potential function satisfies the Laplace equation and, consequently, is expressed in Cartesian coordinates as a series expansion over harmonic polynomials:

$$\Phi(x,y) = V\mathrm{Re}\left[\sum_{N=0}^{\infty} A_N \frac{(x+\mathrm{i}y)^N}{r_0^N}\right] \quad (1)$$

Where, $V$ is amplitude of RF voltage, Re is the real part of the complex value, $r_0$ is "field radius," which is the radius of a circle inscribed between the rods and $A_N$ is the dimensionless amplitude of a 2N-pole field.

SIMION 8.0 was used to calculate the reference potential arrays (unscaled) for each voltage applied to electrodes of the ion trap, using a finite-difference method of grid computing (FDM). The output potential array (PA) files were subsequently used as input to the AXSIM software [7, 23]. Two RF signals with opposite phase were applied to $x$ and $y$ electrode pairs, and RF trapping fields was created in $x$-$y$ plane. Furthermore, an AC signal out of phase was applied to $x$ electrode pairs. During ion trajectory simulations, the magnitude of the grid potentials

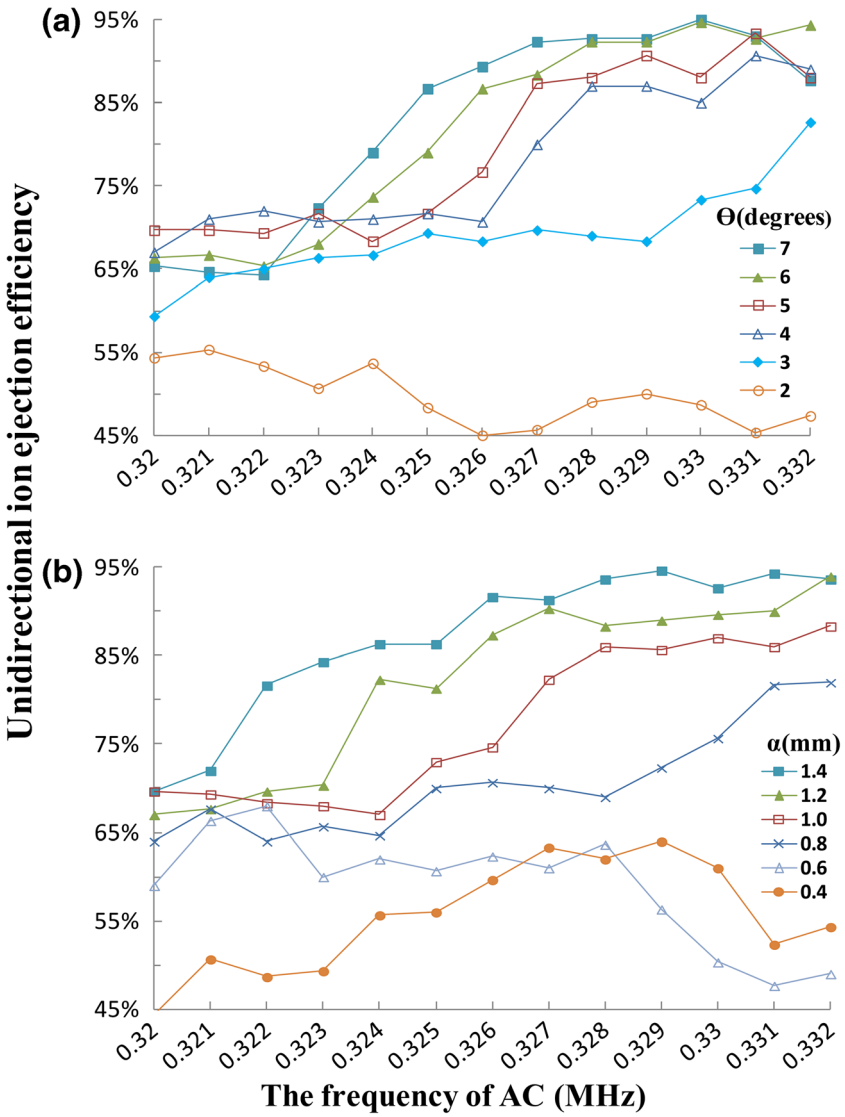


**Figure 5.** Unidirectional ion ejection efficiency as a function of frequency of AC in different A-HreLITs: (**a**) one-way rotated A-HreLIT with different $\theta$; (**b**) one-way stretched A-HreLIT with different $\alpha$

was rescaled according to the magnitude of the applied voltages (RF, AC) to each electrode pairs, and the electric fields- $\varphi_x^{RF}(x,y)$, $\varphi_y^{RF}(x,y)$,$\varphi_x^{AC}(x,y)$, and $\varphi_y^{AC}(x,y)$ were computed via linear interpolation of these grid potentials. Numerical simulations of ion trajectories were performed using the AXSIM software with a fixed 7.815 ns time step to integrate the equations of ion motion as shown below:

$$\frac{d^2x}{dt^2} - \frac{e}{m}\left[V_{RF}(\omega_{RF}t)\frac{\partial\varphi_x^{RF}(x,y)}{\partial x} + V_{AC}(\omega_{AC}t)\frac{\partial\varphi_x^{AC}(x,y)}{\partial x}\right] = 0 \quad (2)$$

$$\frac{d^2y}{dt^2} - \frac{e}{m}\left[V_{RF}(\omega_{RF}t)\frac{\partial\varphi_y^{RF}(x,y)}{\partial y} + V_{AC}(\omega_{AC}t)\frac{\partial\varphi_y^{AC}(x,y)}{\partial y}\right] = 0 \quad (3)$$

$$V_{DE} = -1,500 \text{ volts} \quad (4)$$

Where, m/e is the mass-to-charge ratio of ion, $V_{RF}$ and $V_{AC}$ are the magnitude of the RF voltage and the AC voltage respectively, $w_{RF}$ and $w_{AC}$ are the corresponding angular frequencies. In this case, two detection planes were mounted outside of $x$ electrode pairs (one detection plane for $x^+$ and the other for $x^-$ electrode) and placed 5 mm away from $x$ electrode pairs to avoid the influence of the detection voltage on the trapping field. $V_{DE}$ indicated a negative high voltage applied to the detection plane.

In ion trajectory simulations, ion motion was simulated with random collisions of ions with helium buffer gas at a pressure of 1.0 mTorr and temperature of 300 K using a hard sphere collision model.

## *Simulation of Mass Analysis*

In this study, the HreLIT was operated using the technique of mass selective instability scan and resonance ejection. The main RF power supply was sine wave with fixed frequency (1.0 MHz), and mass analysis was performed by scanning the amplitude of RF signal (with a scan speed of 1500 Th/s). During mass analysis, an excitation signal AC of sine waveform with a particular frequency was applied to excite ions

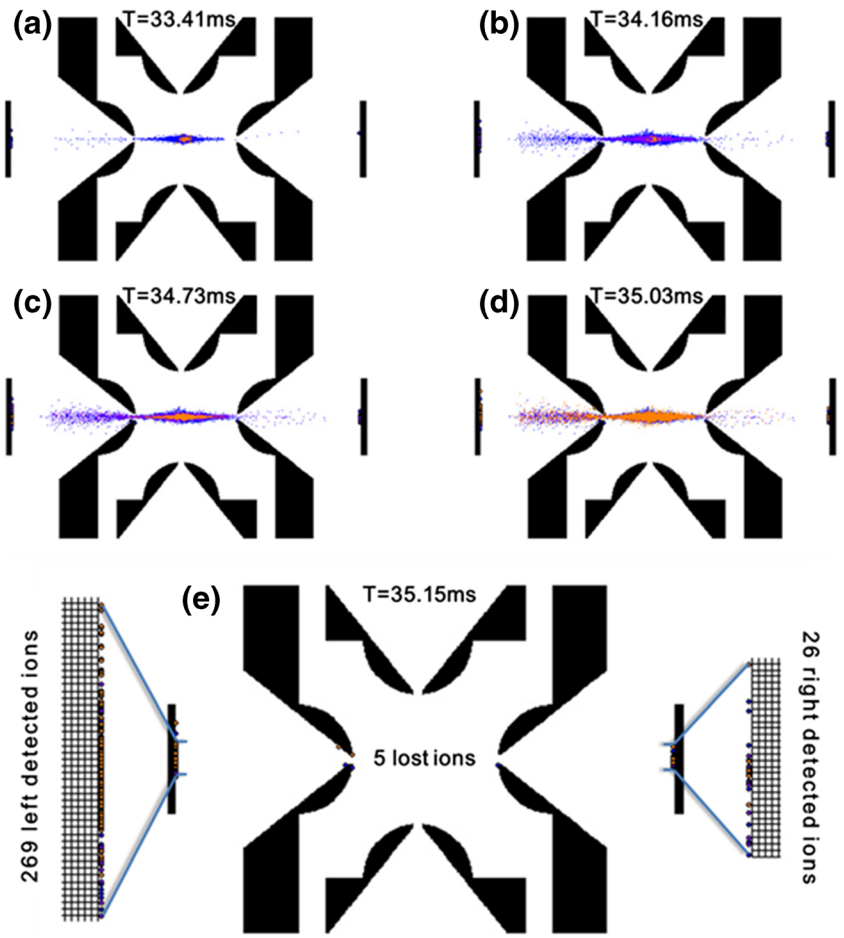


**Figure 6.** Five snapshots of the radial position of an ion population in one-way stretched A-HreLIT with $\alpha = 1.1$ mm over a period of the ions ejection. The ion population include 100 ions of *m/z* 609(blue dots), 100 ions of *m/z* 610(purple dots), and 100 ions of *m/z* 611 (orange dots). (**a**), (**b**), (**c**), (**d**), and (**e**) represents the radial position of 300 ions at different time of $T = 33.41$, 34.16, 34.73, 35.03, and 35.15 ms, respectively. The frequency of AC equals 0.328 MHz in this case

having the same secular frequency. In this case, the amplitude and frequency of AC were critical for the performance of A-HreLIT.

In simulation, the modeled ion populations were comprised of 300 ions (*m/z* 609 Th, 610 Th, 611 Th, each type with a number of 100). The initial position of ions was randomly chosen from a Gaussian distribution around the geometric center of ion trap with a 0.1-mm standard deviation, and the initial energy of ions was around 0 eV with a 0.1-eV deviation. During mass analysis, the termination time and location of ions were recorded and, consequently, mass spectrum and conditions of ion ejection could be obtained. The mass resolution was estimated from the spectrum peak width, unidirectional ion detection efficiency equaled the ratio between number of ions that ejected to one of detection planes and total number of ions (i.e., 300).

## Results and Discussion

### *Geometry Optimization of HreLIT*

The two types of A-HreLITs in this work were designed from the corresponding HreLIT, respectively. So the electrode geometry of two types of HreLITs were first optimized, and then A-HreLIT based on the optimized HreLIT were built, and the changed parts of the structure and asymmetric geometric parameters were both marked in red in Fig. 1(c), (d).

For both types of HreLITs, the slots for ion ejection created some serious nonlinear electric fields because of field penetration inside the slots [24]. To compensate for this serious nonlinear electric fields, a classical method called "stretch" [3] was used in the two types of HreLITs.

Mass resolution versus electrode displacement distance for the two types of HreLIT were shown in Fig. 2, and the amplitude of field distortions was provided for some points in this curve. The mass resolution was estimated from spectrum peak width; the amplitude and frequency of AC voltage were optimized for each stretch distance. For two-slot HreLIT, the high-order fields were predominantly induced by increasing of $r_x$, and simulation results showed that good mass resolution was obtained when $r_x = 5.2$ mm. While for four-slot HreLIT, the high-order fields were predominantly induced by increasing of $r_0$, and the simulation results indicated that an optimum $r_0 = 4.8$ mm leads to good mass resolution.

### *Potential Distribution in A-HreLIT*

With a traditional balanced RF power supply (positive potential 1 V across $x$ rods and negative potential − 1 V across $y$ rods), asymmetric trapping fields were generated in the two types of A-HreLIT. The electric field distributions for different parameters were calculated. Fig. 3(a), (b) showed multipole components A1/A2, A3/A2, A4/A2, and A6/A2 for different rotation angle $\theta$ and different one-way stretch distance $\alpha$ in the two types of A-HreLITs, respectively. For two types of A-HreLITs, the amplitudes of dipole and hexapole components increased approximately proportional to the value of asymmetric geometric parameters $\theta$ (or $\alpha$). While, other high-order electric fields (A4 and A6) remained a low level with the increasing of $\theta$ (or $\alpha$).

Equipotential lines of the two types of A-HreLIT were calculated by SIMION and shown in Fig. 4. The $y$ electrodes

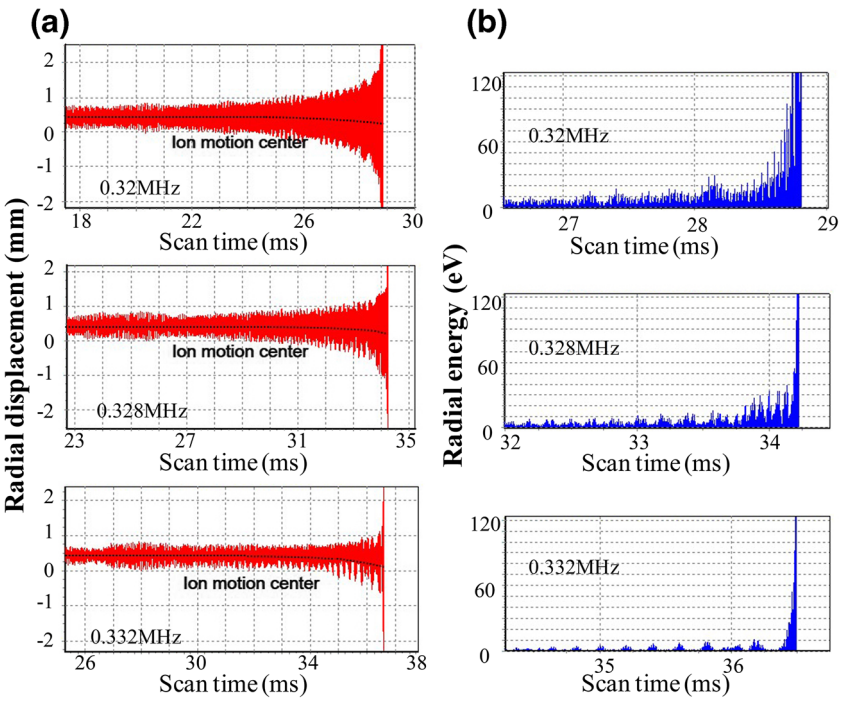


**Figure 7.** The one-way stretched A-HreLIT with $\alpha = 1.1$ mm: (**a**) simulation of ion trajectory in $x$-direction and (**b**) simulation of radial energy of ion vibrations at three different frequencies of AC

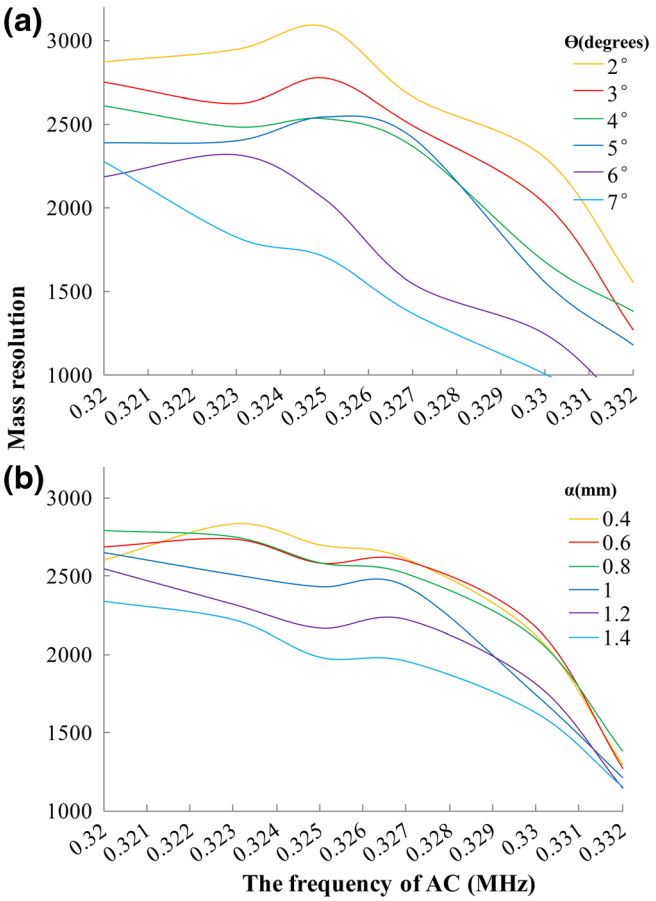


Figure 8. Mass resolution as a function of the frequency of AC in two types of A-HreLITs: (**a**) the one-way rotated A-HreLITs with different $\theta$; (**b**) the one-way stretched A-HreLITs with different $\alpha$

had a potential of 1 V, while the $x$ electrodes had a potential of − 1 V. The calculated equipotential lines showed that the trapping field center was displaced towards one of $x$ electrode pairs. In this case, ions would be accumulated at the center of the trapping field and closer to one of $x$ electrode pairs than the other before ion ejection. Thus, the unidirectional ion ejection occurred during ion resonance ejection.

## *Unidirectional Ion Ejection in A-HreLIT*

During simulation, it was found that the frequency of AC was a critical parameter to unidirectional ion ejection efficiency. The frequency of AC varied from 0.320 to 0.332 MHz, and the amplitude of AC was carefully adjusted until it could eject all ions from the ion trap. Figure 5(a), (b) showed the unidirectional ion ejection efficiency versus frequency of AC for each A-HreLIT with different $\theta$ and $\alpha$, respectively. For one-way rotated A-HreLIT with $\theta \leq 2°$ and one-way stretched A-HreLIT with $\alpha \leq 0.6$ mm, unidirectional ion ejection did not occur. In contrast, when $\theta > 2°$ and $\alpha > 0.6$ mm, unidirectional ion ejection efficiency significantly increased with increasing of $\theta$ (or $\alpha$). In this case, with the frequency of AC increasing, unidirectional ion ejection efficiency also increased significantly and even arrived at more than 90%.

For one-way stretched A-HreLIT with $\alpha = 1.1$ mm, Fig. 6 showed five snapshots of the radial position for 300 ions in the trapping volume over a period of ion ejection when the frequency of AC equaled 0.328 MHz. Similar result was observed in the one-way rotated A-HreLIT with an optimal $\theta$. The center of ion vibration was displaced away from the geometrical center and ions were ejected predominantly through the negative $x$ electrode. It was obvious that most ions were ejected to

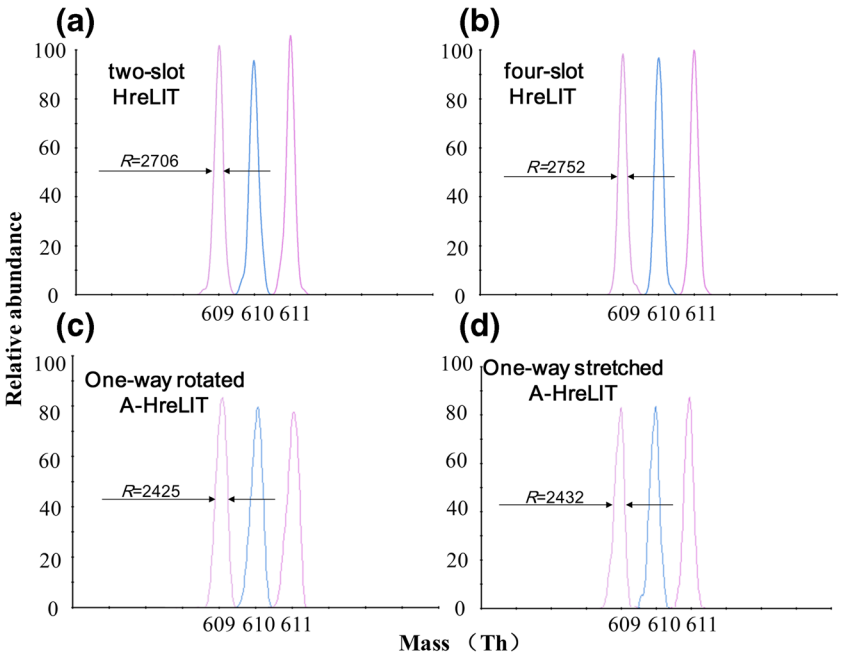


Figure 9. Mass spectrum of simulation for two types of HreLITs and two corresponding types of A-HreLITs: (**a**) two-slot HreLIT with $r_x$ = 5.2 mm; (**b**) four-slot HreLIT with $r_0 = 4.8$ mm; (**c**) one-way rotated A-HreLIT with $\boldsymbol{\theta} = 4°$; (**d**) one-way stretched A-HreLIT with $\alpha = 1$ mm

the detection plane in the negative $x$-direction, while few ions reached the detection plane in the positive $x$-direction. Besides, there were five ions lost by striking the electrodes of ion trap. The estimation of unidirectional ion ejection efficiency in this case was $U = 269/300 = 89.7\%$.

Ion trajectories during resonance excitation were also calculated in two dimensions, and results were shown in Fig. 7(a). The ion trajectories showed a position displacement nearly 0.5 mm away from the origin of coordinate system centered on $x = 0$ just before ion ejection as a result of effects of the asymmetric fields introduced by asymmetric geometries. During ion resonance, ion motion center shifted slightly to the negative $x$ direction with the vibration amplitude of ion increasing, which resulted in ion preferential ejection. Figure 7(b) showed the corresponding ion radial kinetic energy at three different AC frequencies. It was found that the growth rate of ion radial kinetic energy was greater when the frequency of AC was higher. The fast increase in ion kinetic energy means that ions could approach the ejection slots with kinetic energy sufficient for overcoming field distortions near the slot and avoid ejection delay [7, 17], which leads to better analytical performance (including unidirectional ion ejection efficiency and mass resolution).

### *Mass Resolution*

Mass resolution is very important for an ion trap, and so, it is necessary to obtain a considerable mass resolution and high unidirectional ion ejection efficiency simultaneously. For each A-HreLIT with different $\theta$ and $\alpha$, the mass resolution versus the frequency of AC was studied and the results were presented in Fig. 8(a), (b), respectively. Generally, the mass resolution showed a slow downward trend with increasing of asymmetric geometric parameter ($\theta$ or $\alpha$). For one-way rotated A-HreLITs with $\theta > 5°$ and one-way stretched A-HreLITs with $\alpha >$ 1.2 mm, mass resolution showed a downward trend when frequency of AC increased from 0.32 to 0.332 MHz. Mass resolution sharply decreased when the frequency of AC was higher than 0.329 MHz, and mass resolution maintained at a fairly high level when the frequency of AC = 0.328 MHz.

It was expected that unidirectional ion ejection of A-HreLIT arrived at about 90%, while maintaining a considerable mass resolution. Thus, when ion unidirectional ejection efficiency and mass resolution were both taken into account, a compromise should be made and the optimum frequency of AC would be 0.328 MHz.

Figure 9 shows the simulated mass spectrum for two types of HreLIT and two types of A-HreLITs. During mass spectrum simulation, ions were placed in central area of HreLIT for mass analysis in conventional RF mode, and the amplitude of AC signal was optimized for best resolution. For A-HreLIT, the frequency of AC of 0.328 MHz was chosen for high unidirectional ion ejection efficiency and the amplitude of AC was optimized for best resolution at the same time. Figure 9(c), (d) shows the simulated mass spectrum for two types of A-HreLIT. The simulation results indicated that mass resolution of A-HreLIT was slightly lower than that of the corresponding HreLIT, but still maintained a considerably high-mass resolution. Besides, it was worth noting that ion unidirectional ejection efficiency of nearly 90% was achieved in both two types of A-HreLITs.

## Conclusions

In this work, asymmetric trapping fields were generated in two types of A-HreLITs for unidirectional ion ejection. In this case, the center of ion vibration was displaced away from the geometrical center of A-HreLITs and ions were ejected predominantly through one of $x$ electrode pairs. The current investigation has demonstrated that ion detection efficiency could be improved significantly in A-HreLIT mass spectrometer with only one detector, while maintaining a considerably high-mass resolution, which made the A-HreLIT suitable for developing miniaturized mass spectrometer with good analytical performance. Yet, all results in this work were achieved using computer numerical simulation approaches. Constructing real A-HreLIT mass spectrometer and test the performance of unidirectional ion ejection and mass resolution in experiment would be our next work.

## Funding Information

This study is supported by and funded by the Natural Science Foundation of China (61601314).

## References

1. Hager, J.W.: A new linear ion trap mass spectrometer. Rapid Commun. Mass Spectrom. **16**, 512–526 (2002)
2. Hager, J.W.: Off-resonance excitation in a linear ion trap. J. Am. Soc. Mass Spectrom. **20**, 443–450 (2009)
3. Schwartz, J.C., Senko, M.W., Syka, J.E.P.: A two-dimensional quadrupole ion trap mass spectrometer. J. Am. Soc. Mass Spectrom. **13**, 659–669 (2002)
4. Ouyang, Z., Wu, G.X., Song, Y.S., Li, H.Y., Plass, W.R., Cooks, R.G.: Rectilinear ion trap: concepts, calculations, and analytical performance of a new mass analyzer. Anal. Chem. **76**, 4595–4605 (2004)
5. Song, Q.Y., Kothari, S., Senko, M.A., Schwartz, J.C., Amy, J.W., Stafford, G.C., Cooks, R.G., Ouyang, Z.: Rectilinear ion trap mass spectrometer with atmospheric pressure interface and electrospray ionization source. Anal. Chem. **78**, 718–725 (2006)
6. Li, X.X., Jiang, G.Y., Luo, C., Xu, F.X., Wang, Y.Y., Ding, L., Ding, C.F.: Ion trap array mass analyzer: structure and performance. Anal. Chem. **81**, 4840–4846 (2009)
7. Sudakov, M.Y., Apatskaya, M.V., Vitukhin, V.V., Trubitsyn, A.A.: A new linear ion trap with simple electrodes. J. Anal. Chem. **67**, 1057–1065 (2012)
8. Xiao, Y., Ding, Z., Xu, C., Dai, X., Fang, X., Ding, C.-F.: Novel linear ion trap mass analyzer built with triangular electrodes. Anal. Chem. **86**, 5733–5739 (2014)
9. Jiang, D., Jiang, G.Y., Li, X.X., Xu, F.X., Wang, L., Ding, L., Ding, C.F.: Printed circuit board ion trap mass analyzer: its structure and performance. Anal. Chem. **85**, 6041–6046 (2013)
10. Li, X.X., Zhang, X.H., Yao, R.J., He, Y., Zhu, Y.Y., Qian, J.: Design and performance evaluation of a linear ion trap mass analyzer featuring half round rod electrodes. J. Am. Soc. Mass Spectrom. **26**, 734–740 (2015)

11. Gao, L., Song, Q.Y., Patterson, G.E., Cooks, R.G., Ouyang, Z.: Handheld rectilinear ion trap mass spectrometer. Anal. Chem. **78**, 5994–6002 (2006)
12. Peng, Y., Austin, D.E.: New approaches to miniaturizing ion trap mass analyzers. Trac-Trends Analytical Chemistry. **30**, 1560–1567 (2011)
13. Blain, M.G., Riter, L.S., Cruz, D., Austin, D.E., Wu, G.X., Plass, W.R., Cooks, R.G.: Towards the hand-held mass spectrometer: design considerations, simulation, and fabrication of micrometer-scaled cylindrical ion traps. Int. J. Mass Spectrom. **236**, 91–104 (2004)
14. Schwartz, J.C., Syka, J.E.P., Jardine, I.: High-resolution on a quadrupole ion trap mass-spectrometer. J. Am. Soc. Mass Spectrom. **2**, 198–204 (1991)
15. Splendore, M., Marquette, E., Oppenheimer, J., Huston, C., Wells, G.: A new ion ejection method employing an asymmetric trapping field to improve the mass scanning performance of an electrodynamic ion trap. Int. J. Mass Spectrom. **191**, 129–143 (1999)
16. Ding, C.F., Konenkov, N.V., Douglas, D.J.: Quadrupole mass filters with octopole fields. Rapid Commun. Mass Spectrom. **17**, 2495–2502 (2003)
17. Remes, P.M., Syka, J.E.P., Kovtoun, V.V., Schwartz, J.C.: Insight into the resonance ejection process during mass analysis through simulations for improved linear quadrupole ion trap mass spectrometer performance. Int. J. Mass Spectrom. **370**, 44–57 (2014)
18. Zheng, O.Y., Badman, E.R., Cooks, R.G.: Characterization of a serial array of miniature cylindrical ion trap mass analyzers. Rapid Commun. Mass Spectrom. **13**, 2444–2449 (1999)
19. Badman, E.R., Johnson, R.C., Plass, W.R., Cooks, R.G.: A miniature cylindrical quadrupole ion trap: simulation and experiment. Anal. Chem. **70**, 4896–4901 (1998)
20. Patterson, G.E., Guymon, A.J., Riter, L.S., Everly, M., Griep-Raming, J., Laughlin, B.C., Zheng, O.Y., Cooks, R.G.: Miniature cylindrical ion trap mass spectrometer. Anal. Chem. **74**, 6145–6153 (2002)
21. Sekiguchi, H., Matsushita, K., Yamashiro, S., Sano, Y., Seto, Y., Okuda, T., Sato, A.: On-site determination of nerve and mustard gases using a field-portable gas chromatograph-mass spectrometer. Forensic Toxicology. **24**, 17–22 (2006)
22. Wang, Y.Z., Huang, Z.J., Jiang, Y., Xiong, X.C., Deng, Y.L., Fang, X., Xu, W.: The coupling effects of hexapole and octopole fields in quadrupole ion traps: a theoretical study. J. Mass Spectrom. **48**, 937–944 (2013)
23. Zeleny, J.: The electrical discharge from liquid points, and a hydrostatic method of measuring the electric intensity at their surfaces. Phys. Rev. **3**, 69–91 (1914)
24. March, R.E.: Quadrupole ion traps. Mass Spectrom. Rev. **28**, 961–989 (2009)